Review

Cell PRESS

Structure and Function of the Pre-mRNA Splicing Machine

Joseph Sperling,[1] Maia Azubel,[2] and Ruth Sperling[3],*
[1]Department of Organic Chemistry, The Weizmann Institute of Science, Rehovot 76100, Israel
[2]Department of Structural Biology, Stanford University School of Medicine, Stanford, CA 94305-5126, USA
[3]Department of Genetics, The Hebrew University of Jerusalem, Jerusalem 91904, Israel
*Correspondence: sperling@cc.huji.ac.il
DOI 10.1016/j.str.2008.08.011

Most eukaryotic pre-mRNAs contain non-coding sequences (introns) that must be removed in order to accurately place the coding sequences (exons) in the correct reading frame. This critical regulatory pre-mRNA splicing event is fundamental in development and cancer. It occurs within a mega-Dalton multicomponent machine composed of RNA and proteins, which undergoes dynamic changes in RNA-RNA, RNA-protein, and protein-protein interactions during the splicing reaction. Recent years have seen progress in functional and structural analyses of the splicing machine and its subcomponents, and this review is focused on structural aspects of the pre-mRNA splicing machine and their mechanistic implications on the splicing of multi-intronic pre-mRNAs. It brings together, in a comparative manner, structural information on spliceosomes and their intermediates in the stepwise assembly process in vitro, and on the preformed supraspliceosomes, which are isolated from living cell nuclei, with a view of portraying a consistent picture.

Introduction

Eukaryotic pre-mRNAs are transcribed in the cell nucleus by RNA polymerase II (pol II), and must undergo several posttranscriptional modifications before their export to the cytoplasm as functional mRNAs. These processing events include 5'-end capping, 3'-end processing, splicing, and editing. Most pre-mRNAs contain intervening sequences (introns) that must be removed in order to place the coding sequences (exons) in a protein-reading frame. The precise removal of introns from pre-mRNAs by the pre-mRNA splicing machine is, therefore, an essential step in the regulation of gene expression. The mechanism of the chemical transformations involved in this critical processing event, known as pre-mRNA splicing, has been extensively worked out based on studies in vitro, mainly of pre-mRNAs composed of two exons and an intervening intron (Brow, 2002; Burge et al., 1999; Will and Lührmann, 2006). However, the regulation of splicing and alternative splicing of the multi-intronic pre-mRNAs transcribed in vivo is still not well understood, particularly from the standpoint of the structure-function relationship of the spliceosome—the macromolecular machine that catalyzes the splicing reactions. A large body of literature describing high-resolution structures of individual components and domains of the spliceosome has been published and reviewed (Auweter et al., 2006; Clery et al., 2008; Stefl et al., 2005). This review is focused on the overall architecture of the pre-mRNA splicing machine, though at a lower resolution, emphasizing the implications of its structural aspects on the mechanism of the process itself.

Splicing and Spliceosome Assembly In Vitro

The accuracy and efficiency of pre-mRNA splicing is attributed to a number of trans-acting factors, which include the five spliceosomal small nuclear ribonucleoprotein complexes (U1, U2, U4, U5, and U6 snRNPs) (Tycowski et al., 2006) and several non-snRNP protein splicing factors, as well as to cis-acting sequence elements. The latter include 5' and 3' splice sites,

a branch point, and a polypyrimidine tract. Splicing enhancers and silencers are additional control elements that play an important role in both constitutive and alternative splicing, by interacting with the serine/arginine-rich (SR) protein splicing factors (Bourgeois et al., 2004; Sanford et al., 2005).

Studies in vitro revealed that RNA splicing proceeds through a mechanism involving two trans-esterification reactions (Figure 1). It occurs in the spliceosome, a dynamic machine that undergoes several changes in interactions and conformations. The assembly of the 60S spliceosome in vitro occurs in a stepwise manner (reviewed in Brow, 2002; Will and Lührmann, 2001, 2006). This process involves a series of interactions among the five major snRNPs, as well as a number of non-snRNP splicing factors, which are dynamically recruited to the spliceosome when an exogenous pre-mRNA is added to a crude nuclear extract. The spliceosomal snRNPs participate in splice-site recognition and thus play an essential role in splicing through cooperative RNA-RNA interactions between the snRNAs themselves and with the pre-mRNA (Brow, 2002; Burge et al., 1999; Staley and Guthrie, 1998; Tycowski et al., 2006).

Density gradient centrifugation and native gel electrophoresis revealed at least four intermediate complexes (E, A, B, and C) in the assembly process in vitro of the major class of spliceosomes (U2 spliceosomes) (Figure 2). For the catalytic activation of the spliceosome, complex B undergoes a structural change, forming an intricate network of interactions between U6 and U2 snRNAs with the pre-messenger RNA molecule, which together constitute part of the catalytic core of the spliceosome. The activated complex B undergoes the first catalytic step of splicing, which generates complex C. Complex C undergoes the second catalytic step, after which the postspliceosomal intron-containing complex is dismantled and the mRNA product is released (Nilsen, 1998; Staley and Guthrie, 1998). A minor group of spliceosomes (U12 spliceosomes), composed of U11, U12, U4atac, U6atac (replacing U1, U2, U4, and U6 snRNPs, respectively), U5 snRNP, and several
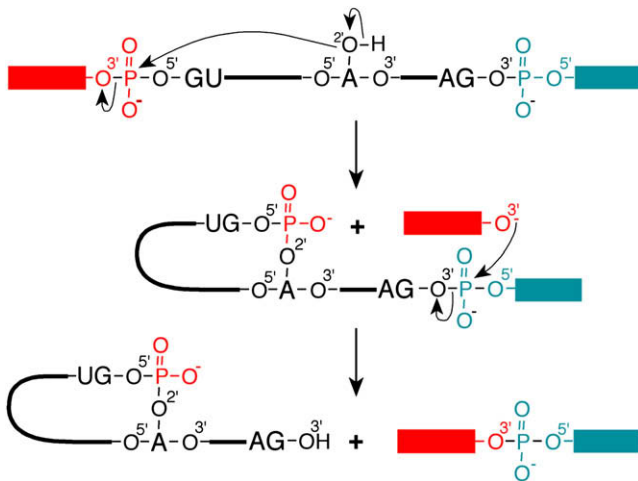
Figure 1. Mechanism of RNA Splicing
First step: The 2′ hydroxyl of a specific adenosine base at the branch site of a pre-mRNA becomes nucleophilic and makes a nucleophilic substitution type 2 (SN2) attack on the phosphodiester moiety at the 5′ splice site (marked in red). Two intermediates are formed: the 5′ exon in a free form (red) and the 3′ exon-intron moiety in a lariat form. Second step: In a second SN2-type reaction, the free 3′ hydroxyl anion of the 5′ exon attacks the phosphodiester moiety at the 3′ splice site (marked in blue) to yield the spliced RNA and the spliced-out intron in a lariat form.

Figure 2. Schematic Presentation of the Stepwise Spliceosome Assembly Pathway In Vitro
When pre-mRNA is added to a crude nuclear extract of cells (color code as in Figure 1) complex E is formed by the binding of U1 snRNP (green) to the 5′ splice site of the pre-mRNA. Complex A is then formed by an ATP-dependent interaction of U2 snRNP with the branch site. Addition of the U4/U6.U5 tri-snRNP gives rise to complex B. This step is followed by the release of the U1 and U4 snRNPs and the remodeling of complex B to yield the splicing-active complex C. For simplification, binding of hnRNP, SR, and other spliceosomal proteins to various cis-acting elements of the pre-mRNA, which occur during the splicing reaction, are not shown.

proteins, are assembled on the minority of introns that also have U12-specific cis elements at the pre-mRNA (Tycowski et al., 2006).

Recent molecular and genetic studies emphasized the importance of conformational changes within the spliceosome for splicing regulation and quality control during the splicing process. These studies also highlighted the role of RNA helicases in controlling the fidelity of the splicing reaction (Mayas et al., 2006; Query and Konarska, 2006; Staley and Guthrie, 1998; Valadkhan, 2007), and revealed the existence of mutually incompatible conformational states of the active site during the two steps of splicing (Konarska et al., 2006; Rhode et al., 2006). Although such remodeling of the spliceosome is likely to be controlled by an extensive and dynamic network of protein-protein, RNA-RNA, and protein-RNA interactions, these transitions, as discussed below, do not necessarily require large-scale structural changes (namely, changes in the overall shape of the complex), but can be accounted for by local conformational changes (Nilsen, 1998; Rhode et al., 2006; Valadkhan, 2007).

Structural Studies of Spliceosomes and Their Subcomponents Assembled In Vitro
X-ray and NMR Studies of Spliceosomal Subcomponents
In terms of resolution and accuracy, X-ray crystallography is highly instrumental for understanding molecular architectures. Nevertheless, the use of this technique for structural studies of large biological complexes, such as the mega-Dalton splicing complexes, is hampered by the requirements for large quantities of homogenous material. Therefore, the high-resolution structures that have thus far been resolved in the splicing field by X-ray and NMR are confined to individual proteins or to spliceosomal domains rather than to the larger assembled complexes (reviewed in Auweter et al., 2006; Clery et al., 2008; Stefl et al., 2005). Highlights of this literature are described in this review
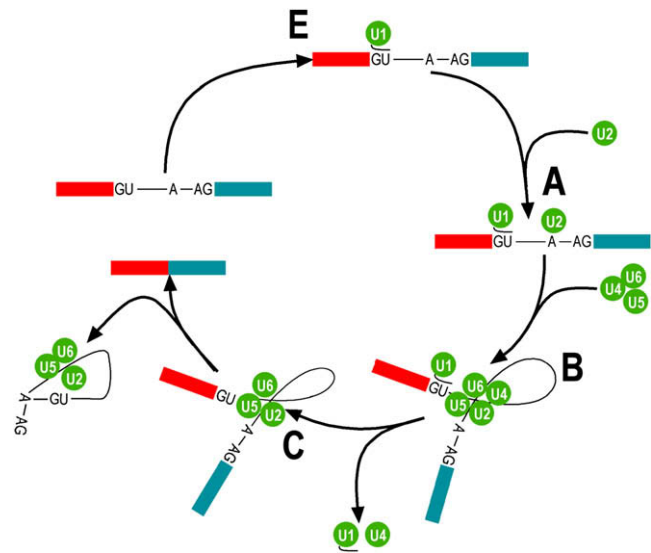
when relevant to its main focus, which addresses the structural analysis of larger and functional splicing complexes.

The spliceosomal snRNAs constitute a key element in the functioning of the splicing machine, and their small sizes make them amenable to NMR studies. Butcher and colleagues have solved several of U snRNA structures, with emphasize on U2 and U6 snRNAs in light of their proposed role in catalysis (Blad et al., 2005; Butcher and Brow, 2005; McManus et al., 2007; Sashital et al., 2007). An important aspect of U2 snRNA function is its base-pairing interaction with the pre-mRNA branch site, which positions a bulged adenosine to serve as the nucleophile in the first chemical step of pre-mRNA splicing. In accordance with this proposed mechanism, X-ray (Lin and Kielkopf, 2008) and NMR (Newby and Greenbaum, 2002) structures of RNA oligonucleotide duplexes composed of the pseudouridylated U2 snRNA and the branchpoint consensus sequences, revealed an extrahelical adenosine at the adenosine branch point.

Protein-RNA and protein-protein interactions also underlie the structure and function of the splicing machine. One of the most common protein-folds that mediate protein-RNA interactions is the RNA recognition motif (RRM), also termed RNA binding domain (RBD). Structural analyses by X-ray crystallography and NMR helped provide a molecular basis for the RRM-RNA recognition. The dual ability of proteins with this motif to interact both with proteins and RNA plays a key role in splicing. Structural studies suggest that the surface exposed to the RNA could determine whether an interaction occurs. This is in accordance with the observed variations of sequence specificity in different interactions (reviewed in Clery et al., 2008; Maris et al., 2005).
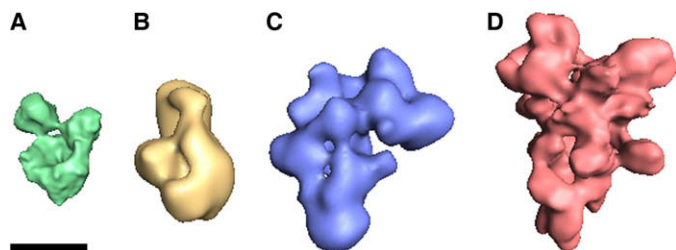
Figure 3. EM Structural Analyses of Spliceosomal snRNPs
Three-dimensional image reconstruction of spliceosomal snRNPs by EM single-particle technique. Bar represents 10 nm.
(A) U1 snRNP (Stark et al., 2001)
(B) U4/U6 snRNPs (Sander et al., 2006)
(C) U5 snRNP (Sander et al., 2006)
(D) U4/U6.U5 tri-snRNP (Sander et al., 2006)

Each of the U1, U2, U4, and U5 snRNPs share a common core of a heptameric Sm protein complex, which is bound as a ring-shaped structure to an Sm binding sequence in the respective snRNA (Kambach et al., 1999). A similar heptameric ring complex, termed like-Sm (LSm), binds to a specific site in the U6 snRNA (Will and Lührmann, 2001). In addition, each snRNP contains specific proteins, as revealed by biochemical analyses and confirmed by mass spectrometry (MS) (Will and Lührmann, 2001). The structure of the RBD1 domain of U1A, one of the specific proteins of the U1 snRNP, was solved either in the presence of a 21-nt RNA hairpin at a resolution of 1.92 Å (Oubridge et al., 1994), or by NMR (Lu and Hall, 1997) and by X-ray crystallography as a free domain at a resolution of 1.8 Å (Rupert et al., 2003). In the case of U2 snRNP, the structure of several protein-RNA and protein-protein complexes has been studied. U2B″-U2A′ in a ternary complex with stem loop IV of U2 snRNA has been resolved by X-ray crystallography (Price et al., 1998). Also, the U2 snRNP-specific protein P14.SF3b has been partially resolved both by X-ray crystallography (Schellenberg et al., 2006) and NMR (Kuwasako et al., 2007).

The U2 auxiliary factor proteins U2AF[65] and U2AF[35] are required for the binding of U2 snRNP to the pre-mRNA. Structural studies of subcomplexes representing interactions of these proteins include the following: (i) a complex between the central domain of U2AF[35] and the proline-rich region of U2AF[65] (Kielkopf et al., 2001); (ii) individual RBD domains of U2AF[65] by NMR (Ito et al., 1999) and by X-ray crystallography (Thickman et al., 2007); (iii) U2AF[65] RBD complexed with splicing factor SF1 (Selenko et al., 2003) and the binding of SF1 to the branch point (Liu et al., 2001); and (iv) U2AF[65] RBD complexed with a heptameric uridine RNA oligonucleotide (Sickmier et al., 2006). These studies showed that U2AF[65] makes an unusual number of RNA contacts via intervening water molecules and flexible side chains, which enable its binding to different, including poorly conserved, polypyrimidine-tract sequences.

Structural studies of subcomponents of U5.U4/U6 tri-snRNP were also performed. The structure of the U5 snRNP 15K-specific protein was reported at a resolution of 1.4 Å (Reuter et al., 1999), as was its structure in complex with the GYF domain of U5 snRNP 52K protein (Nielsen et al., 2007). The structure of cyclophilin H complexed with a peptide derived from the U4/U6 60K-specific protein revealed a novel protein-protein interaction (Reidt et al., 2003). Finally, the structure of U5.U4/U6 15.5K-specific protein in the presence of the 5′-end stem loop of U4 snRNA has been elucidated (Vidovic et al., 2000).

Structures of wild-type and mutant Prp (precursor RNA processing) proteins were reported mainly in yeast (Prp 19 [Van der Kooi et al., 2006]; Prp 24 [Bae et al., 2007]; WW domain of Prp 40 bound to Prp8 [Wiesner et al., 2002]; mutant Prp 18 [Jiang et al., 2000]). Studies of mutations and comparisons between

different organisms revealed interesting information about mechanism. A typical example is the C-terminal domain of Prp 8, whose structure was resolved in both yeast (Pena et al., 2007) and *Caenorhabditis elegans* (Zhang et al., 2007). Both studies show that the C-terminal domain is involved in protein-protein interaction. Mutations in the C-terminal domain of human Prp8 are linked to the RP13 form of retinitis pigmentosa, and they also disrupt its interaction with Brr2 and Snu114. Thus, it has been proposed that dysfunction of this protein-protein platform might underlie a plausible molecular explanation for retinitis pigmentosa (Pena et al., 2007).

SR proteins constitute an important component of the non-snRNP protein splicing factors. Known to be involved in regulating and selecting splice sites, SR proteins play a key role in alternative splicing (Bourgeois et al., 2004). The structures of the RRM of SRp20 and 9GB, as well as the structure of the RRM of SRp20 in complex with 4 nt RNA sequence (5′CAUC3′), have been solved (Hargous et al., 2006). The latter structure revealed that only the 5′ cytosine is recognized in a specific way. The structure of RRM2 of ASF/SF2 bound to RNA revealed a new way of binding to the RNA (Tintaru et al., 2007). The polypyrimidine tract binding protein (PTB) involved in splicing regulation and alternative splicing and in multiple aspects of RNA processing is composed of four RRMs; the structure of each with and without RNA was solved, providing insight into its diverse functional roles (reviewed in Auweter and Allain, 2008). The structure of UAP56, an essential splicing factor and mRNA export factor, was solved at 1.9 Å. The structure of this DExD/H-box protein suggests that it posses both helicase and ATPase activities (Zhao et al., 2004). These structures are highlighted examples of available high-resolution information on individual spliceosomal components that reveal partial interactions, which might be further incorporated into lower-resolution structures of larger complexes.

Structural Studies of Spliceosomal snRNPs by Cryo-Electron Microscopy

High-resolution structural information is not yet available for any of the splicing complexes. Nevertheless, cryo-electron microscopy (cryo-EM) has been instrumental in the three-dimensional (3D) image reconstruction of certain splicing subcomplexes, though at a lower resolution (Stark and Lührmann, 2006). Figure 3 depicts structures of four snRNP complexes, all drawn to the same scale for size comparison.

U1 snRNP is the smallest spliceosomal snRNP. It is composed of U1 snRNA, the seven Sm proteins, and three specific proteins (U1-A, U1-70K, and U1-C). Its 3D structure was determined by cryo-EM single-particle technique at a resolution of 10 Å (Stark et al., 2001) (Figure 3A). U2 snRNP consists of U2 snRNA, the seven Sm proteins, and about 15 U2-specific proteins, grouped
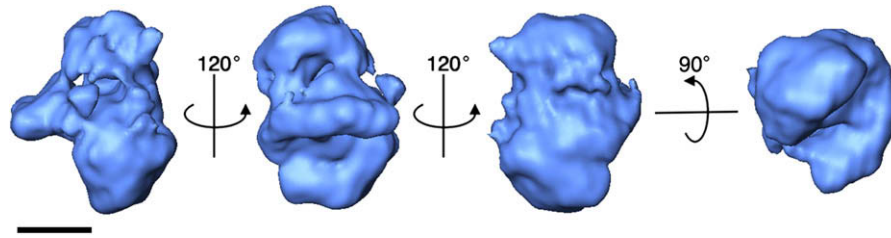
Figure 4. Structure of the In Vitro-Assembled Complex C
Different views of a surface representation of in vitro-assembled complex C, reconstructed at 30 Å resolution from cryonegatively stained images and contoured to an estimated mass of 2.6 MDa (Jurica et al., 2004). Bar represents 10 nm.

in splicing factor 3a and 3b (SF3a and SF3b), which assemble sequentially to form the U2 snRNP (Stark and Lührmann, 2006). The structure of U2 snRNP has not yet been determined, but the structure of SF3b was determined by cryo-EM single-particle technique at 10 Å resolution (Golas et al., 2003). U11/U12 di-snRNP is part of the minor spliceosome. Although U11 and U12 snRNPs are functionally equivalent to U1 and U2 snRNPs in the major spliceosome, they differ from the two latter complexes in that they form a stable complex, whereas U1 and U2 snRNPs do not. The U11/U12 di-snRNP share with U2 snRNP the seven SF3b proteins, whereas most of the other proteins are different. Cryo-EM structural analyses of U11/U12 di-snRNP at ∼12 Å resolution revealed that in order to accommodate the structure of SF3b within the structure of U11/U12 di-snRNP, the structure of the former has to undergo major conformational changes (Golas et al., 2005). With respect to size and mass, the U5 snRNP is a major component of the spliceosome. The human 20S U5 snRNP consists of the U5 snRNA, seven Sm proteins, and nine U5 snRNP-specific proteins (reviewed in Will and Lührmann, 2006). Structural analysis of U5 snRNP at 26–32 Å resolution by cryonegative staining revealed a triangular structure (Sander et al., 2006) (Figure 3C). The U4/U6.U5 tri-snRNP complex contains the U4/U6 and U5 snRNAs and 29 distinct proteins (reviewed in Will and Lührmann, 2006). Structural analyses by cryo-EM at 19–24 Å resolution revealed elongated triangular particles (Sander et al., 2006) (Figure 3D). Structural analysis of U4/U6 di-snRNP at ∼40 Å resolution showed two distinct globular domains connected by a bridge (Sander et al., 2006) (Figure 3B).

Intermediate Splicing Complexes Assembled In Vitro
Three-dimensional reconstructions of a number of intermediates in the pathway of the spliceosome assembly in vitro were per-

formed. To allow comparison between these structures (Figures 4–6) and the structure of the native spliceosome, which is discussed below (Figure 7), all structures are drawn to the same scale. The C-complex spliceosome, which contains three of the five spliceosomal U snRNPs (U2, U5, and U6 snRNPs), was resolved at a resolution of 30 Å using cryonegative staining and the sandwich method (Jurica et al., 2004). The 27 × 22 × 24 nm structure revealed three major domains, at a threshold that accentuates the division into domains (Figure 4). The structure of a U5.U2/U6 spliceosome complex from fission yeast was resolved by cryo-EM single-particle technique at a resolution of 29 Å (Ohi et al., 2007) (Figure 5). This complex, which sedimented at 37S, was obtained by tandem affinity purification under nonphysiological conditions. Mass measurements by scanning transmission electron microscopy (STEM) revealed a mass of 2.0 MDa, yet the cumulative mass of proteins identified by MS analysis of this complex revealed a mass of 3.0 MDa (Ohi et al., 2002). A better agreement with the measured mass was obtained by summing up the masses of U2, U5, and U6 snRNPs and the nineteen complex (NTC), found in this splicing complex, which gave a mass of 2.2 MDa. The structure of the U5.U2/U6 spliceosome complex depicts distinct domains that contact each other at the center of the complex, with an overall dimension of 30 × 20 × 18 nm (Ohi et al., 2007). The structure of this complex is similar to that of the in vitro-assembled mammalian complex C (Figure 4).

The structure of the precatalytic spliceosomal complex B lacking the U1 snRNP (BΔU1) was solved at a resolution of 40 Å using cryonegative staining and the sandwich method (Boehringer et al., 2004). The 3D reconstruction revealed a structure with a flexible head domain. The structure, having maximal dimensions of 37 × 27 × 17 nm, is more extended in one direction and narrower in a perpendicular direction (Figure 6). Comparison of the structure of BΔU1 with that of
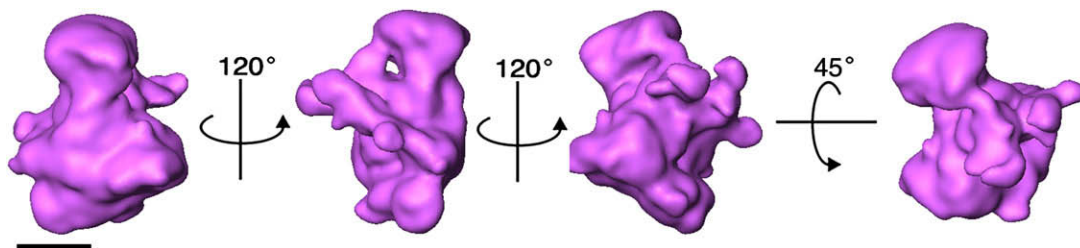

Figure 5. Structure of *Schizosaccharomyces pombe* U5.U2/U6 Splicing Complex
Different views of a surface representation of the *S. pombe* U5.U2/U6 splicing complex, reconstructed at 29 Å resolution from cryoimages and contoured to a STEM-measured mass of 2.0 MDa (Ohi et al., 2007). Bar represents 10 nm.
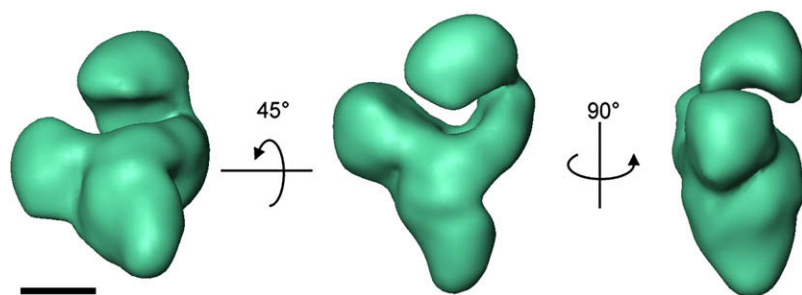
Figure 6. Structure of In Vitro-Assembled Complex BΔU1

Different views of a surface representation of in vitro-assembled complex BΔU1, reconstructed at 40 Å resolution from cryonegatively stained images and contoured to an estimated mass of 5.5 MDa (Boehringer et al., 2004). Bar represents 10 nm.

tri-snRNP led the authors to suggest that tri-snRNP is placed at the lower triangular domain of BΔU1. Analysis of negatively stained spliceosomal A complex at 40–50 Å resolution was recently performed (Behzadnia et al., 2007). This complex, isolated by double-affinity purification, contained the U1 and U2 snRNPs and had an asymmetric shape structure with overall dimensions of 23 × 20 × 19.5 nm.

Splicing Complexes Isolated from Intact Mammalian Cells—Supraspliceosomes
Isolation of Supraspliceosomes
An alternative, top-down approach for the isolation of physiologically significant splicing complexes from mammalian cell nuclei was initiated by Sperling et al. (1985). Isolation conditions were optimized whereby over 85% of ^{3}H-labeled pol II transcripts could be released to a nuclear supernatant. Fractionation of such nuclear supernatants in sucrose or glycerol gradients revealed that the labeled pol II transcripts sedimented at the 200S region in the gradient (Sperling et al., 1985). Visualization by EM of aliquots from fractions across the gradient revealed a peak of large tetrameric structures, having overall dimensions of 50 × 50 nm (Figure 8A), which cosedimented at 200S with the peak of the ^{3}H-labeled pol II transcripts (Spann et al., 1989). Analyses of the distribution across the gradient of specific RNA transcripts (e.g., CAD, DHFR, and actin), as well as of the general population of the nuclear polyadenylated RNAs, showed that they all sedimented at the 200S region (Spann et al., 1989; Sperling et al., 1985). These 200S complexes, initially called large nuclear RNP complexes, were termed supraspliceosomes.

Supraspliceosomes were shown to contain all five spliceosomal snRNPs as integral components of the complex (Miriami et al., 1995; Sperling and Sperling, 1998; Yitzhaki et al., 1996), as well as a large number of non-snRNP protein splicing factors (Miriami et al., 1995; Sperling and Sperling, 1998; Yitzhaki et al., 1996). It is physiologically significant that all phosphorylated SR proteins, which are required for spliceosome assembly and alternative splicing, are predominantly associated within the supraspliceosome (Yitzhaki et al., 1996). A remarkable feature of supraspliceosomes is that they package pre-mRNA transcripts of different sizes and of different number of introns into complexes of a unique size and hydrodynamic properties, indicating their universal nature (Azubel et al., 2006; Miriami et al., 1994; Spann et al., 1989; Sperling et al., 1997; Sperling and Sperling, 1998; Yitzhaki et al., 1996).

Structural Studies of the Supraspliceosome
The complexity and large size of the supraspliceosome made EM the method of choice for its structural analysis. Three-dimensional image reconstruction of individual supraspliceosomes by automated electron tomography of negatively stained (Sperling et al., 1997) and of frozen hydrated complexes (Medalia et al., 2002) showed the supraspliceosome as forming a closed structure, 50 × 50 × 35 nm in size, composed mainly of four similar subcomplexes. Mass measurements by STEM showed that the supraspliceosome has a mass of 21 MDa, and each of its main subcomplexes has a mass of 4.8 MDa (Müller et al., 1998). Further STEM and cryo-EM studies revealed that the subcomplexes of the supraspliceosome are interconnected, presumably by the pre-mRNA (Medalia et al., 2002; Müller et al., 1998). These observations led to the working hypothesis that each supraspliceosome packs one pre-mRNA and can therefore be responsible for its posttranscriptional processing, where each of its four major subcomplexes represents a spliceosome that can splice the intron wound around it.

Isolation and Characterization of Native Spliceosomes
The four subcomplexes of the supraspliceosome are interconnected in a flexible way and may thus adopt different angular settings, which impose a significant restriction on reaching high resolution in EM image analyses. Therefore, a method was developed to prepare and isolate the monomeric spliceosomal subcomplexes from supraspliceosomes, by specific cleavage of the general population of pre-mRNAs, while keeping the snRNAs within these subcomplexes intact (Azubel et al., 2004, 2006). The resulting complexes were purified by centrifugation in a glycerol gradient, where they sedimented at the 60–70S region (Azubel et al., 2006). Northern blot analysis revealed that, like the supraspliceosome, the subcomplexes contained the full complement of the five spliceosomal snRNAs (Azubel et al., 2006). Importantly, the subcomplexes and supraspliceosomes were functional in splicing (Azubel et al., 2006). Hence, the subcomplexes were termed native spliceosomes.

Structural Analysis of Native Spliceosomes by the Cryo-EM Single-Particle Technique
The isolation of native spliceosomes and their relative stability enabled their 3D cryo-EM structural analysis by the single-particle technique at a resolution of 20 Å (Azubel et al., 2004) (Figure 7). The structure revealed an elongated globular particle made up of two distinct subunits. This finding is consistent with previous STEM mass measurements, which revealed two major, equally populated, distinct groups of small particles with masses of 1.5 MDa and 3.1 MDa, which together are close in mass to the 4.8 MDa native spliceosome (Müller et al., 1998). The two subunits are interconnected with a tunnel running between them, which is large enough to allow the pre-mRNA to pass through. The other
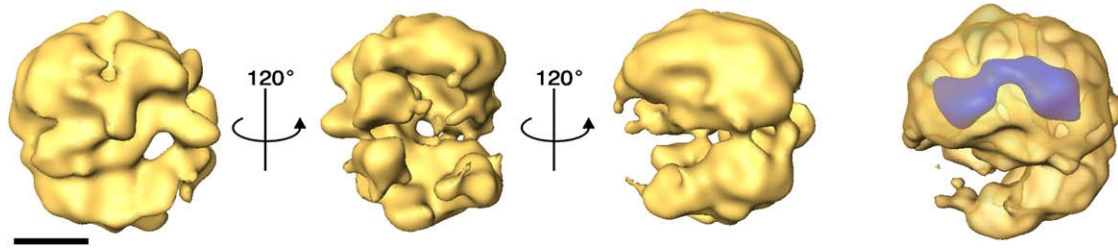
Figure 7. Structure of the Native Spliceosome
Different views of a surface representation of the native spliceosome reconstructed at 20 Å resolution from cryoimages (Azubel et al., 2004). The structure was contoured to a STEM-measured mass of 4.8 MDa (Müller et al., 1998). In the right panel, high-threshold rendering (blue surface) shows the high-density mass region, which represents the stable RNAs within the structure of the native spliceosome. The large subunit of the native spliceosome is thus a suitable candidate to harbor the five spliceosomal snRNPs. Adapted from Azubel et al. (2004). Bar represents 10 nm.

side of the native spliceosome exposes a cavity that could provide a place to transiently store the pre-mRNA. The large subunit was shown to be a suitable candidate to accommodate the five spliceosomal snRNPs, because the high density regions were confined to the large subunit (Figure 7, far right image) (Azubel et al., 2004).

Organization of the Native Spliceosomes within the Supraspliceosome
To address how the native spliceosomes are arranged within the intact supraspliceosome, EM structural analysis and reconstruction of the native spliceosomes in the context of the intact particle was performed. It was shown that the small subunits reside in the center of the supraspliceosome and their edges form a right angle, thus facilitating close contacts between the small subunits generating a four-fold pattern (Figure 8B) (Cohen-Krausz et al., 2007). A good correlation was obtained between the structure of the isolated native spliceosome, solved by cryo-EM (Azubel et al., 2004), and that of the native spliceosome within the intact supraspliceosome (Cohen-Krausz et al., 2007).

Biological Significance of the Supraspliceosome
Is the tetrameric structure of the supraspliceosome biologically significant? Due to the particular mode of organization of the supraspliceosome into a large multicomponent structure, it can be regarded as a biological self-assembly system. Whereas various oligomeric forms of such systems may be observed under non-physiological conditions; under physiological conditions, the biologically relevant active macromolecular complex prevails. Furthermore, when a biological self-assembly system is composed of nucleic acids and proteins, not only that the biologically relevant complex prevails under physiological conditions, but it requires the presence of both the nucleic acid and protein components. In this context, it is important to note that supraspliceosomes were isolated under physiological conditions, and the pre-mRNA was shown to be essential for their assembly (Spann et al., 1989; Sperling et al., 1985). Namely, when the pre-mRNA was cleaved, supraspliceosomes irreversibly dissociated into native spliceosomes (Azubel et al., 2006). Furthermore, the isolated supraspliceosomes were shown to be functional (Azubel et al., 2006). Additional important information, although seemingly circumstantial, is in support of the notion that the supraspliceosome is a biologically significant entity. (i) Specific pre-mRNA transcripts, as well as their splicing intermediates and fully spliced RNAs, prevail in supraspliceosomes (Miriami et al., 1994; Spann et al., 1989; Sperling and Sperling, 1998; Sperling et al., 1985). (ii) Supraspliceosomes harbor all known splicing factors; particularly, the phosphorylated forms of the SR protein are predominantly associated with tetrameric supraspliceosomes (Yitzhaki et al., 1996). (iii) STEM mass measurements revealed a relatively uniform mass for the supraspliceosome (21.1 ± 1.6 MDa; n = 400), and for the native spliceosome (4.8 ± 0.5; n = 510) (Müller et al., 1998). Further support for the concept of a biologically significant supraspliceosomal complex was inferred from a study showing that U2/U6 snRNA base pairing, which characterizes active spliceosomes assembled in vitro, were found in complexes sedimenting between 150S and 300S but not in 60S complexes (Wassarman and Steitz, 1993). Also, analysis of pol II transcripts in situ, in cells grown in tissue culture, revealed that they are assembled in supraspliceosomes (Iborra et al., 1998).

Comparison of Splicing Complexes Assembled In Vitro and In Vivo
Splicing complexes assembled in vitro and in vivo are both highly dynamic macromolecular complexes that undergo several conformational changes and alterations in RNA-RNA, protein-RNA, and protein-protein interactions during the splicing reaction. With respect to mass and dimensions, the fully in vitro-assembled 60S spliceosome appears to be similar to the native spliceosome, which is derived from the in vivo-assembled tetrameric supraspliceosome. Although the mass of the 60S in vitro-assembled spliceosome has not yet been directly determined, the structure of the splicing complex BΔU1 (Boehringer et al., 2004) was presented using extreme threshold that enclosed a volume that corresponded to either 6.5 or 4.5 MDa. The authors then proposed that 5.5 MDa (the averaged mass) corresponded to the mass of the splicing complex BΔU1. Another estimate, based on sedimentation velocity of the 60S spliceosome, gave 4.9 MDa (Müller et al., 1998). In comparison, the mass of the native spliceosome, directly measured by STEM, is 4.8 MDa (Müller et al., 1998). In this respect, the supraspliceosome could be regarded as being composed of four spliceosomes. Yet, the complexes assembled in vivo differ from those assembled in vitro in at least two conceptual aspects: one pertains to their assembly pathway, the other pertains to the way they are expected to splice multi-intronic pre-mRNAs.
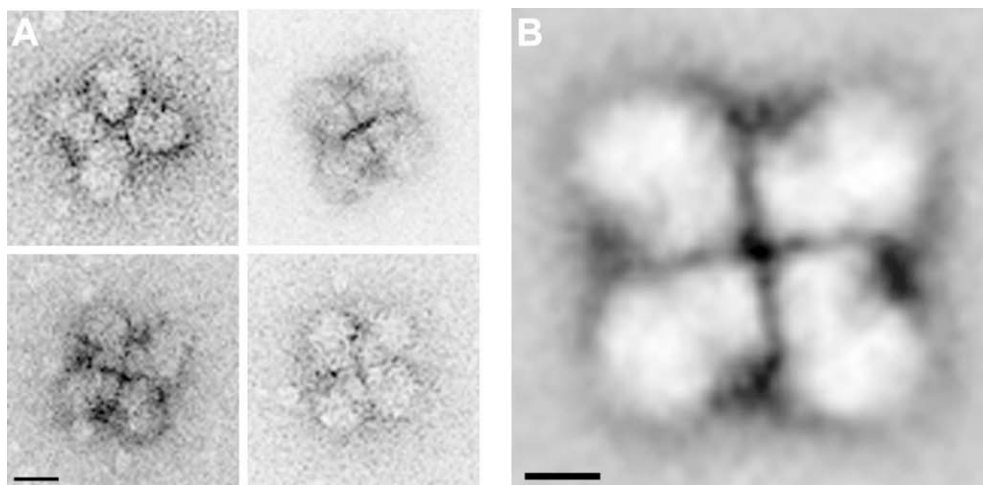
Figure 8. Electron Microscopy of the Supraspliceosome
(A) A gallery of EM images of supraspliceosomes each composed of four subcomplexes—native spliceosomes. Bar represents 20 nm.
(B) Intact supraspliceosomes were classified by Correspondence Analysis and Hierarchical Ascendant Classification. One of the classes is depicted showing the close contact between neighboring substructures in the center of the supraspliceosome. Adapted from Cohen-Krausz et al. (2007). Bar represents 10 nm.

The assembly of the spliceosome in vitro was shown to proceed in a stepwise manner (Brow, 2002; Staley and Guthrie, 1998), whereas the assembly of newly transcribed pre-mRNAs into supraspliceosomes in vivo appeared to involve preformed complexes (Azubel et al., 2006; Iborra et al., 1998; Stevens et al., 2002). Furthermore, the assembly pathway in vitro is characterized by major changes in composition (e.g., only three of the five spliceosomal snRNPs are part of the active C complex). However, both the supraspliceosome and the native spliceosome contain all five spliceosomal snRNPs (Azubel et al., 2006). This finding, together with the ability to isolate a functional "penta-snRNP" complex from yeast (Stevens et al., 2002), further highlights the important role of large, preformed complexes in pre-mRNA splicing in vivo. The apparent discrepancy between the notion of a stepwise assembly pathway of the spliceosome in vitro and the occurrence of a preformed splicing complex in vivo has been explained by a "holospliceosome" model, in which the sequential complexes represent ordered modulations within the in vivo-assembled spliceosome without the loss of components (Brow, 2002). It has also been pointed out that such distinct complexes, which represent intermediate states in spliceosome assembly in vitro, may not occur in vivo (Nilsen, 2002; Stevens et al., 2002).

The assembly pathways of supraspliceosomes in vivo and that of spliceosomes assembled in vitro also differ in the sense that the former occurs cotranscriptionally in the nucleus, whereas the assembly process in vitro occurs when a full-length pre-mRNA is interacting with the spliceosomal components present in a nuclear extract. We suggest that these two likely distinct pathways might lead to different local minima in the respective free energy profiles, which could result in the assembly of slightly different complexes. Alternatively, the observed changes in composition between intermediate complexes assembled in vitro, which are not found in native spliceosomes and supraspliceosomes, might be due to the lack of specific components present in native spliceosomes, which help keep the latter particles together. In this context it should be noted that the

in vitro-assembled splicing complexes were usually isolated in the presence of heparin, which could have caused partial dissociation of components (Deckert et al., 2006) (e.g., the splicing complex BΔU1 was isolated in the presence of heparin [Boehringer et al., 2004], whereas U1 snRNP was included in complex B when heparin was omitted [Deckert et al., 2006]).

Analysis by MS of several of the in vitro-assembled splicing complexes and their subcomplexes yielded a large arsenal of proteins, some of which were already identified as splicing factors and some of which are new (reviewed in Jurica and Moore, 2003; Nilsen, 2003; Will and Lührmann, 2006). Yet, the cumulative mass of proteins found by MS in the splicing complexes highly exceeds the respective estimated or measured mass of these complexes (see above), indicating that further refinement of the MS results is required. Recently, MS analyses of complexes isolated from HeLa cells by a modification of the supraspliceosome protocol (Miriami et al., 1994) revealed over 300 proteins, including a large number of splicing factors and also several proteins not found in spliceosomes assembled in vitro (Chen et al., 2007). It is reassuring that most of the proteins identified as components of the supraspliceosome (Raitskin et al., 2001, 2002; Sperling and Sperling, 1998; Yitzhaki et al., 1996) were validated through these MS analyses. However, further analyses of well-defined high-quality preparations are necessary to obtain a more accurate picture of the supraspliceosome proteome.

Because the stepwise assembly pathway of the spliceosome in vitro involves major changes in composition, it could have been assumed that the changes in interactions that occur within this complex during the splicing reaction involve major structural rearrangements. However, such compositional changes were not found in supraspliceosomes and native spliceosomes. It is therefore plausible that the changes in base-pairing interactions within the native spliceosome are likely accompanied by less dramatic global structural changes than anticipated, and with less dramatic compositional changes than those found in the in vitro-assembled spliceosome. In support of this notion is the
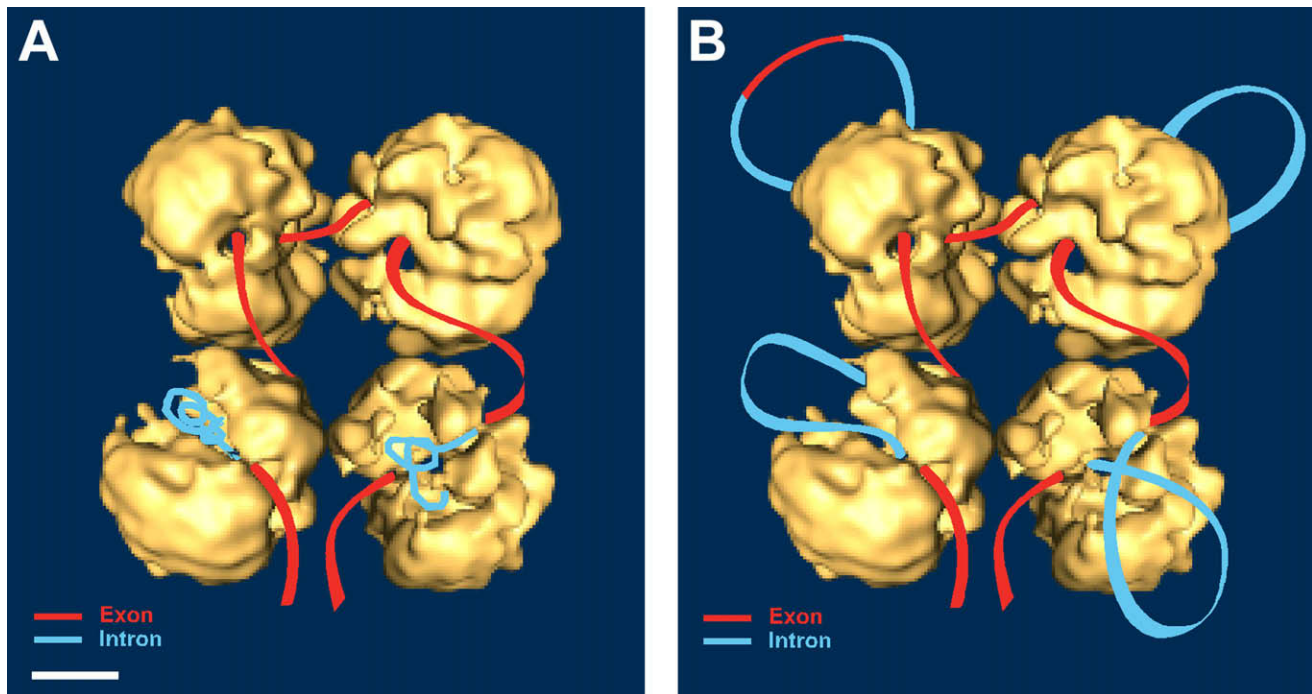
Figure 9. The Supraspliceosome Model
Schematic models of the supraspliceosome in which the pre-mRNA (introns in blue, exons in red) is connecting four native spliceosomes. The supraspliceosome presents a platform onto which the exons can be aligned and splice junctions can be checked before splicing occurs.
(A) The pre-mRNA that is not being processed is folded and protected within the cavities of the native spliceosome.
(B) When a staining protocol that allows visualization of nucleic acids was used, RNA strands and loops were seen emanating from the supraspliceosomes (Müller et al., 1998). Under these conditions the RNA kept in the cavity is proposed to unfold and loop-out. In the looped-out scheme an alternative exon is depicted in the upper left corner. From Azubel et al. (2006). Bar represents 10 nm.

fact that the structure of the native spliceosome was determined by cryo-EM single-particle technique at a resolution of 20 Å (Azubel et al., 2004), suggesting that the structural changes that occur in vivo are more subtle than those that could be resolved at this resolution.

Splicing of Multi-intronic Pre-mRNAs
Most of our knowledge of the biochemistry and mechanism of splicing has been derived from studies on spliceosomes assembled in vitro on pre-mRNAs comprising one intron flanked by two exons. Yet, because the majority of mammalian pre-mRNAs are multi-intronic, it can be anticipated that in mammalian cell nuclei the pre-mRNAs would be assembled in multi-spliceosome complexes. Therefore, the finding that splicing complexes isolated from live mammalian cells are assembled in supraspliceosomes is not surprising, and it is reassuring that the native spliceosome—the building block of these structures—resembles the in vitro-assembled spliceosome.

Alternative splicing, whereby different combinations of exons are spliced together to produce different mRNAs from a single-copy gene, should also be considered in the context of the structure-function relationship of the splicing machine. It has been estimated that 40%–75% of the ~25,000 human genes undergo alternative splicing, thereby increasing the coding potential of the human genome by more than one order of magnitude (Brett et al., 2002; Garcia-Blanco et al., 2004; Modrek and Lee, 2002; Srebrow and Kornblihtt, 2006). Regulated splicing, as well as

constitutive splicing, operates through the combinatorial interplay of positive and negative regulatory signals present in the pre-mRNA, which are recognized by trans-acting factors, the most studied of which are members of the hnRNP and SR protein families (Bourgeois et al., 2004; Sanford et al., 2005).

To account for the necessity to splice multi-intronic pre-mRNAs, a modular multispliceosome model that extrapolates from the in vitro-assembled spliceosome has been implied in the published literature. Namely, a pre-mRNA having N introns would require N spliceosomes for its processing. Such a model can account for splicing regulation within each individual spliceosome, taking advantage of the interplay between splicing factors and the respective cis elements they recognize. Yet, this model does not explain how splicing regulation and communication between spliceosomes, as well as quality control of multi-intronic transcripts, might be achieved.

The supraspliceosome, by contrast, presents a closed-structure model composed of four native spliceosomes connected by the pre-mRNA. A critical experiment in support of this arrangement showed that cleavage of the pre-mRNA yielded functional native spliceosomes that could be reconstituted into supraspliceosomes by incubation with exogenously added pre-mRNAs (Azubel et al., 2004, 2006). In this configuration, the supraspliceosome acts as a multiprocessor machine that can simultaneously splice four introns—not necessarily in a consecutive manner (Figure 9). In this schematic model, which was based on structural studies (Azubel et al., 2004, 2006; Cohen-Krausz

et al., 2007; Müller et al., 1998), each of the four subcomplexes of the supraspliceosome is presented by the 20-Å resolution structure of the native spliceosome (Azubel et al., 2004). The small subunit of each native spliceosome, proposed to harbor non-snRNP components such as SR proteins and hnRNP proteins, is placed at the center of the supraspliceosome (Cohen-Krausz et al., 2007). This configuration allows communication between the native spliceosomes, which is a crucial element for regulated alternative splicing and for quality control of the resulting mRNAs. This setting places the large subunit of each native spliceosome, where catalysis by the penta-snRNP presumably takes place, in the periphery of the supraspliceosome. Thus, the supraspliceosome presents a platform on which splice junctions could be checked before introns excision. An attractive feature of such a machine is that it allows rearrangement of splice junction combinations to select the appropriate ones. This way it comprises an important tool to ensure the fidelity of splicing and alternative splicing.

Splicing of a multi-intronic pre-mRNA can be facilitated by the translocation of the pre-mRNA through the complex in a "rolling model" fashion. After processing of four introns, the RNA rolls in to place a new subset of introns in the correct position for their processing. The possibility that splicing occurs cotranscriptionally (Neugebauer, 2002) could help explain how pre-mRNAs having an exceptionally large number of introns (e.g., dystrophin or CAD) can be spliced by the supraspliceosome in a rolling mode. At the other extreme, reconstitution experiments with pre-mRNAs having only one intron indicated that pre-mRNAs having less then four introns are also packaged in supraspliceosomes (Azubel et al., 2006). Thus, the interactions of the RNA with the native spliceosomes per se are presumably sufficient to hold the structure together.

Concluding Remarks

Like many biological machines that act on polymeric substrates (e.g., the ribosome, and the RNA and DNA polymerases) the RNA splicing machine is expected to be processive. Yet, introns in multi-intronic transcripts are spliced at different rates and in a nonsequential mode (Wetterberg et al., 1996), which is characteristic of a distributive process. The proposed mode of action of the supraspliceosome helps resolve this apparent contradiction in the sense that it does not require that processing of the four introns starts and ends simultaneously, while maintaining the processivity of the machine.

In light of the growing realization that biological processes are coupled, it is reassuring that the supraspliceosome harbor additional functional pre-mRNA-processing factors and activities that have not been reported as components of the in vitro-assembled spliceosome. These factors are required for additional processing of pre-mRNA (e.g., the editing enzymes ADAR1 and ADAR2 [Agranat et al., 2008; Raitskin et al., 2001]). It also harbors 3′-end and 5′-end processing components (Raitskin et al., 2002). Thus, the supraspliceosome can account for all aspects of nuclear pre-mRNA-processing activities, including alternative splicing and quality control of the pre-mRNA.

Clearly, for a better understanding of the intricate network of interactions among the components of the splicing machine and how they bring about its function and regulation, it would be necessary to derive structural information at a higher resolution than that presently available. A major factor that interferes with deriving such information is that the isolated supraspliceosomes represent a steady state population, which is intrinsically heterogeneous with respect to its pre-mRNA components and the different stages of the splicing reaction they have reached. Therefore, it would be necessary to develop methods for the preparation and isolation of supraspliceosomes assembled on a single, preselected pre-mRNA at a given stage of the splicing reaction. Current and future development of methods for the stabilization of splicing complexes representing intermediate stages of spliceosomes assembled in vitro should provide high-resolution information on these complexes, and on specific interactions between components within them. It is anticipated that it should be possible to integrate the high-resolution information from both the in vitro and in vivo studies in a complementary and synergistic manner into a coherent mechanistic picture on pre-RNA splicing and its regulation in the cell nucleus.

REFERENCES

Agranat, L., Raitskin, O., Sperling, J., and Sperling, R. (2008). The editing enzyme ADAR1 and the mRNA surveillance protein hUpf1 interact in the cell nucleus. Proc. Natl. Acad. Sci. USA 105, 5028–5033.

Auweter, S.D., and Allain, F.H. (2008). Structure-function relationships of the polypyrimidine tract binding protein. Cell. Mol. Life Sci. 65, 516–527.

Auweter, S.D., Oberstrass, F.C., and Allain, F.H. (2006). Sequence-specific binding of single-stranded RNA: is there a code for recognition? Nucleic Acids Res. 34, 4943–4959.

Azubel, M., Wolf, S.G., Sperling, J., and Sperling, R. (2004). Three-dimensional structure of the native spliceosome by cryo-electron microscopy. Mol. Cell 15, 833–839.

Azubel, M., Habib, N., Sperling, J., and Sperling, R. (2006). Native spliceosomes assemble with pre-mRNA to form supraspliceosomes. J. Mol. Biol. 356, 955–966.

Bae, E., Reiter, N.J., Bingman, C.A., Kwan, S.S., Lee, D., Phillips, G.N., Jr., Butcher, S.E., and Brow, D.A. (2007). Structure and interactions of the first three RNA recognition motifs of splicing factor prp24. J. Mol. Biol. 367, 1447–1458.

Behzadnia, N., Golas, M.M., Hartmuth, K., Sander, B., Kastner, B., Deckert, J., Dube, P., Will, C.L., Urlaub, H., Stark, H., and Lührmann, R. (2007). Composition and three-dimensional EM structure of double affinity-purified, human prespliceosomal A complexes. EMBO J. 26, 1737–1748.

Blad, H., Reiter, N.J., Abildgaard, F., Markley, J.L., and Butcher, S.E. (2005). Dynamics and metal ion binding in the U6 RNA intramolecular stem-loop as analyzed by NMR. J. Mol. Biol. 353, 540–555.

Boehringer, D., Makarov, E.M., Sander, B., Makarova, O.V., Kastner, B., Lührmann, R., and Stark, H. (2004). Three-dimensional structure of a pre-catalytic human spliceosomal complex B. Nat. Struct. Mol. Biol. 11, 463–468.

Bourgeois, C.F., Lejeune, F., and Stevenin, J. (2004). Broad specificity of SR (serine/arginine) proteins in the regulation of alternative splicing of pre-messenger RNA. Prog. Nucleic Acid Res. Mol. Biol. 78, 37–88.

Brett, D., Pospisil, H., Valcárcel, J., Reich, J., and Bork, P. (2002). Alternative splicing and genome complexity. Nat. Genet. 30, 29–30.

Brow, D.A. (2002). Allosteric cascade of spliceosome activation. Annu. Rev. Genet. 36, 333–360.

Burge, C.B., Tuschl, T.H., and Sharp, P.A. (1999). Splicing of precursors to mRNAs by the spliceosomes. In The RNA World, Second Edition, R.F. Gesteland, T.R. Cech, and J.F. Atkins, eds. (Cold Spring Harbor, New York: Cold Spring Harbor Laboratory Press), pp. 525–560.

Butcher, S.E., and Brow, D.A. (2005). Towards understanding the catalytic core structure of the spliceosome. Biochem. Soc. Trans. 33, 447–449.

Chen, Y.I., Moore, R.E., Ge, H.Y., Young, M.K., Lee, T.D., and Stevens, S.W. (2007). Proteomic analysis of in vivo-assembled pre-mRNA splicing complexes expands the catalog of participating factors. Nucleic Acids Res. 35, 3928–3944.

Clery, A., Blatter, M., and Allain, F.H. (2008). RNA recognition motifs: boring? Not quite. Curr. Opin. Struct. Biol. 18, 290–298.

Cohen-Krausz, S., Sperling, R., and Sperling, J. (2007). Exploring the architecture of the intact supraspliceosome using electron microscopy. J. Mol. Biol. 368, 319–327.

Deckert, J., Hartmuth, M., Boehringer, D., Behzadnia, N., Will, C.L., Kastner, B., Stark, H., Urlaub, H., and Lührmann, R. (2006). Protein composition and electron microscopy structure of affinity-purified human spliceosomal B complexes isolated under physiological conditions. Mol. Cell. Biol. 26, 5528–5543.

Garcia-Blanco, M.A., Baraniak, A.P., and Lasda, E.L. (2004). Alternative splicing in disease and therapy. Nat. Biotechnol. 22, 535–546.

Golas, M.M., Sander, B., Will, C.L., Lührmann, R., and Stark, H. (2005). Major conformational change in the complex SF3b upon integration into the spliceosomal U11/U12 di-snRNP as revealed by electron cryomicroscopy. Mol. Cell 17, 869–883.

Golas, M.M., Sander, B., Will, C.L., Lührmann, R., and Stark, H. (2003). Molecular architecture of the multiprotein splicing factor SF3b. Science 300, 980–984.

Hargous, Y., Hautbergue, G.M., Tintaru, A.M., Skrisovska, L., Golovanov, A.P., Stevenin, J., Lian, L.Y., Wilson, S.A., and Allain, F.H. (2006). Molecular basis of RNA recognition and TAP binding by the SR proteins SRp20 and 9G8. EMBO J. 25, 5126–5137.

Iborra, F.J., Jackson, D.A., and Cook, P.R. (1998). The path of transcripts from extra-nucleolar synthetic sites to nuclear pores: transcripts in transit are concentrated in discrete structures containing SR proteins. J. Cell Sci. 111, 2269–2282.

Ito, T., Muto, Y., Green, M.R., and Yokoyama, S. (1999). Solution structures of the first and second RNA-binding domains of human U2 small nuclear ribonucleoprotein particle auxiliary factor (U2AF(65)). EMBO J. 18, 4523–4534.

Jiang, J., Horowitz, D.S., and Xu, R.M. (2000). Crystal structure of the functional domain of the splicing factor Prp18. Proc. Natl. Acad. Sci. USA 97, 3022–3027.

Jurica, M.S., and Moore, M.J. (2003). Pre-mRNA splicing: awash in a sea of proteins. Mol. Cell 12, 5–14.

Jurica, M.S., Sousa, D., Moore, M.J., and Grigorieff, N. (2004). Three-dimensional structure of C complex spliceosomes by electron microscopy. Nat. Struct. Mol. Biol. 11, 265–269.

Kambach, C., Walke, S., Young, R., Avis, J.M., de la Fortelle, E., Raker, V.A., Lührmann, R., Li, J., and Nagai, K. (1999). Crystal structures of two Sm protein complexes and their implications for the assembly of the spliceosomal snRNPs. Cell 96, 375–387.

Kielkopf, C.L., Rodionova, N.A., Green, M.R., and Burley, S.K. (2001). A novel peptide recognition mode revealed by the X-ray structure of a core U2AF35/U2AF65 heterodimer. Cell 106, 595–605.

Konarska, M.M., Vilardell, J., and Query, C.C. (2006). Repositioning of the reaction intermediate within the catalytic center of the spliceosome. Mol. Cell 21, 543–553.

Kuwasako, K., Dohmae, N., Inoue, M., Shirouzu, M., Taguchi, S., Guntert, P., Seraphin, B., Muto, Y., and Yokoyama, S. (2007). Complex assembly mechanism and an RNA-binding mode of the human p14-SF3b155 spliceosomal protein complex identified by NMR solution structure and functional analyses. Proteins 71, 1617–1636.

Lin, Y., and Kielkopf, C.L. (2008). X-ray structures of U2 snRNA-branchpoint duplexes containing conserved pseudouridines. Biochemistry 47, 5503–5514.

Liu, Z., Luyten, I., Bottomley, M.J., Messias, A.C., Houngninou-Molango, S., Sprangers, R., Zanier, K., Kramer, A., and Sattler, M. (2001). Structural basis for recognition of the intron branch site RNA by splicing factor 1. Science 294, 1098–1102.

Lu, J., and Hall, K.B. (1997). Tertiary structure of RBD2 and backbone dynamics of RBD1 and RBD2 of the human U1A protein determined by NMR spectroscopy. Biochemistry 36, 10393–10405.

Maris, C., Dominguez, C., and Allain, F.H. (2005). The RNA recognition motif, a plastic RNA-binding platform to regulate post-transcriptional gene expression. FEBS J. 272, 2118–2131.

Mayas, R.M., Maita, H., and Staley, J.P. (2006). Exon ligation is proofread by the DExD/H-box ATPase Prp22p. Nat. Struct. Mol. Biol. 13, 482–490.

McManus, C.J., Schwartz, M.L., Butcher, S.E., and Brow, D.A. (2007). A dynamic bulge in the U6 RNA internal stem-loop functions in spliceosome assembly and activation. RNA 13, 2252–2265.

Medalia, O., Typke, D., Hegerl, R., Angenitzki, M., Sperling, J., and Sperling, R. (2002). Cryoelectron microscopy and cryoelectron tomography of the nuclear pre-mRNA processing machine. J. Struct. Biol. 138, 74–84.

Miriami, E., Angenitzki, M., Sperling, R., and Sperling, J. (1995). Magnesium cations are required for the association of U small nuclear ribonucleoproteins and SR proteins with pre-mRNA in 200 S large nuclear ribonucleoprotein particles. J. Mol. Biol. 246, 254–263.

Miriami, E., Sperling, J., and Sperling, R. (1994). Heat shock affects 5′ splice site selection, cleavage and ligation of CAD pre-mRNA in hamster cells, but not its packaging in lnRNP particles. Nucleic Acids Res. 22, 3084–3091.

Modrek, B., and Lee, C. (2002). A genomic view of alternative splicing. Nat. Genet. 30, 13–19.

Müller, S., Wolpensinger, B., Angenitzki, M., Engel, A., Sperling, J., and Sperling, R. (1998). A supraspliceosome model for large nuclear ribonucleoprotein particles based on mass determinations by scanning transmission electron microscopy. J. Mol. Biol. 283, 383–394.

Neugebauer, K.M. (2002). On the importance of being co-transcriptional. J. Cell Sci. 115, 3865–3871.

Newby, M.I., and Greenbaum, N.L. (2002). Sculpting of the spliceosomal branch site recognition motif by a conserved pseudouridine. Nat. Struct. Biol. 9, 958–965.

Nielsen, T.K., Liu, S., Lührmann, R., and Ficner, R. (2007). Structural basis for the bifunctionality of the U5 snRNP 52K protein (CD2BP2). J. Mol. Biol. 369, 902–908.

Nilsen, T.W. (1998). RNA-RNA interactions in nuclear pre-mRNA splicing. In RNA structure and function, R.W. Simons and M. Grunberg-Manago, eds. (Cold Spring Harbor, New York: Cold Spring Harbor Laboratory Press), pp. 279–307.

Nilsen, T.W. (2002). The spliceosome: no assembly required? Mol. Cell 9, 8–9.

Nilsen, T.W. (2003). The spliceosome: the most complex macromolecular machine in the cell? Bioessays 25, 1147–1149.

Ohi, M.D., Link, A.J., Ren, L., Jennings, J.L., McDonald, W.H., and Gould, K.L. (2002). Proteomics analysis reveals stable multiprotein complexes in both fission and budding yeasts containing Myb-related Cdc5p/Cef1p, novel pre-mRNA splicing factors, and snRNAs. Mol. Cell. Biol. 22, 2011–2024.

Ohi, M.D., Ren, L., Wall, J.S., Gould, K.L., and Walz, T. (2007). Structural characterization of the fission yeast U5.U2/U6 spliceosome complex. Proc. Natl. Acad. Sci. USA 104, 3195–3200.

Oubridge, C., Ito, N., Evans, P.R., Teo, C.H., and Nagai, K. (1994). Crystal structure at 1.92 A resolution of the RNA-binding domain of the U1A spliceosomal protein complexed with an RNA hairpin. Nature 372, 432–438.

Pena, V., Liu, S., Bujnicki, J.M., Lührmann, R., and Wahl, M.C. (2007). Structure of a multipartite protein-protein interaction domain in splicing factor prp8 and its link to retinitis pigmentosa. Mol. Cell 25, 615–624.

Price, S.R., Evans, P.R., and Nagai, K. (1998). Crystal structure of the spliceosomal U2B″-U2A′ protein complex bound to a fragment of U2 small nuclear RNA. Nature 394, 645–650.

Query, C.C., and Konarska, M.M. (2006). Splicing fidelity revisited. Nat. Struct. Mol. Biol. *13*, 472–474.

Raitskin, O., Cho, D.S., Sperling, J., Nishikura, K., and Sperling, R. (2001). RNA editing activity is associated with splicing factors in lnRNP particles: the nuclear pre-mRNA processing machinery. Proc. Natl. Acad. Sci. USA *98*, 6571–6576.

Raitskin, O., Angenitzki, M., Sperling, J., and Sperling, R. (2002). Large nuclear RNP particles-the nuclear pre-mRNA processing machine. J. Struct. Biol. *140*, 123–130.

Reidt, U., Wahl, M.C., Fasshauer, D., Horowitz, D.S., Lührmann, R., and Ficner, R. (2003). Crystal structure of a complex between human spliceosomal cyclophilin H and a U4/U6 snRNP-60K peptide. J. Mol. Biol. *331*, 45–56.

Reuter, K., Nottrott, S., Fabrizio, P., Lührmann, R., and Ficner, R. (1999). Identification, characterization and crystal structure analysis of the human spliceosomal U5 snRNP-specific 15 kD protein. J. Mol. Biol. *294*, 515–525.

Rhode, B.M., Hartmuth, K., Westhof, E., and Lührmann, R. (2006). Proximity of conserved U6 and U2 snRNA elements to the 5′ splice site region in activated spliceosomes. EMBO J. *25*, 2475–2486.

Rupert, P.B., Xiao, H., and Ferre-D'Amare, A.R. (2003). U1A RNA-binding domain at 1.8 A resolution. Acta Crystallogr. D Biol. Crystallogr. *59*, 1521–1524.

Sander, B., Golas, M.M., Makarov, E.M., Brahms, H., Kastner, B., Lührmann, R., and Stark, H. (2006). Organization of core spliceosomal components U5 snRNA loop I and U4/U6 Di-snRNP within U4/U6.U5 Tri-snRNP as revealed by electron cryomicroscopy. Mol. Cell *24*, 267–278.

Sanford, J.R., Ellis, J., and Caceres, J.F. (2005). Multiple roles of arginine/serine-rich splicing factors in RNA processing. Biochem. Soc. Trans. *33*, 443–446.

Sashital, D.G., Venditti, V., Angers, C.G., Cornilescu, G., and Butcher, S.E. (2007). Structure and thermodynamics of a conserved U2 snRNA domain from yeast and human. RNA *13*, 328–338.

Schellenberg, M.J., Edwards, R.A., Ritchie, D.B., Kent, O.A., Golas, M.M., Stark, H., Lührmann, R., Glover, J.N., and MacMillan, A.M. (2006). Crystal structure of a core spliceosomal protein interface. Proc. Natl. Acad. Sci. USA *103*, 1266–1271.

Selenko, P., Gregorovic, G., Sprangers, R., Stier, G., Rhani, Z., Kramer, A., and Sattler, M. (2003). Structural basis for the molecular recognition between human splicing factors U2AF65 and SF1/mBBP. Mol. Cell *11*, 965–976.

Sickmier, E.A., Frato, K.E., Shen, H., Paranawithana, S.R., Green, M.R., and Kielkopf, C.L. (2006). Structural basis for polypyrimidine tract recognition by the essential pre-mRNA splicing factor U2AF65. Mol. Cell *23*, 49–59.

Spann, P., Feinerman, M., Sperling, J., and Sperling, R. (1989). Isolation and visualization of large compact ribonucleoprotein particles of specific nuclear RNAs. Proc. Natl. Acad. Sci. USA *86*, 466–470.

Sperling, R., and Sperling, J. (1998). The lnRNP particle: a naturally assembled complex of pre-mRNA and splicing factors. In RNP Particles, Splicing and Autoimmune Diseases, J. Schenkel, ed. (Berlin: Springer), pp. 29–47.

Sperling, R., Koster, A.J., Melamed-Bessudo, C., Rubinstein, A., Angenitzki, M., Berkovitch-Yellin, Z., and Sperling, J. (1997). Three-dimensional image reconstruction of large nuclear RNP (lnRNP) particles by automated electron tomography. J. Mol. Biol. *267*, 570–583.

Sperling, R., Sperling, J., Levine, A.D., Spann, P., Stark, G.R., and Kornberg, R.D. (1985). Abundant nuclear ribonucleoprotein form of CAD RNA. Mol. Cell. Biol. *5*, 569–575.

Srebrow, A., and Kornblihtt, A.R. (2006). The connection between splicing and cancer. J. Cell Sci. *119*, 2635–2641.

Staley, J.P., and Guthrie, C. (1998). Mechanical devices of the spliceosome: motors, clocks, springs, and things. Cell *92*, 315–326.

Stark, H., and Lührmann, R. (2006). Cryo-electron microscopy of spliceosomal components. Annu. Rev. Biophys. Biomol. Struct. *35*, 435–457.

Stark, H., Dube, P., Lührmann, R., and Kastner, B. (2001). Arrangement of RNA and proteins in the spliceosomal U1 small nuclear ribonucleoprotein particle. Nature *409*, 539–542.

Stefl, R., Skrisovska, L., and Allain, F.H. (2005). RNA sequence- and shape-dependent recognition by proteins in the ribonucleoprotein particle. EMBO Rep. *6*, 33–38.

Stevens, S.W., Ryan, D.E., Ge, H.Y., Moore, R.E., Young, M.K., Lee, T.D., and Abelson, J. (2002). Composition and functional characterization of the yeast spliceosomal penta-snRNP. Mol. Cell *9*, 31–44.

Thickman, K.R., Sickmier, E.A., and Kielkopf, C.L. (2007). Alternative conformations at the RNA-binding surface of the N-terminal U2AF(65) RNA recognition motif. J. Mol. Biol. *366*, 703–710.

Tintaru, A.M., Hautbergue, G.M., Hounslow, A.M., Hung, M.L., Lian, L.Y., Craven, C.J., and Wilson, S.A. (2007). Structural and functional analysis of RNA and TAP binding to SF2/ASF. EMBO Rep. *8*, 756–762.

Tycowski, K.T., Kolev, N.G., Conard, N.K., Fok, V., and Steitz, J.A. (2006). The ever-growing world of small nuclear ribonucleoproteins. In The RNA World, Third Edition, R.F. Gesteland, T.R. Cech, and J.F. Atkins, eds. (Cold Spring Harbor, New York: Cold Spring Harbor Laboratory Press), pp. 327–368.

Valadkhan, S. (2007). The spliceosome: caught in a web of shifting interactions. Curr. Opin. Struct. Biol. *17*, 310–315.

Vander Kooi, C.W., Ohi, M.D., Rosenberg, J.A., Oldham, M.L., Newcomer, M.E., Gould, K.L., and Chazin, W.J. (2006). The Prp19 U-box crystal structure suggests a common dimeric architecture for a class of oligomeric E3 ubiquitin ligases. Biochemistry *45*, 121–130.

Vidovic, I., Nottrott, S., Hartmuth, K., Lührmann, R., and Ficner, R. (2000). Crystal structure of the spliceosomal 15.5kD protein bound to a U4 snRNA fragment. Mol. Cell *6*, 1331–1342.

Wassarman, D.A., and Steitz, J.A. (1993). A base-pairing interaction between U2 and U6 small nuclear RNAs occurs in >150S complexes in HeLa cell extracts: Implications for the spliceosome assembly pathway. Proc. Natl. Acad. Sci. USA *90*, 7139–7143.

Wetterberg, I., Bauren, G., and Wieslander, L. (1996). The intranuclear site of excision of each intron in Balbiani ring 3 pre-mRNA is influenced by the time remaining to transcription termination and different excision efficiencies for the various introns. RNA *2*, 641–651.

Wiesner, S., Stier, G., Sattler, M., and Macias, M.J. (2002). Solution structure and ligand recognition of the WW domain pair of the yeast splicing factor Prp40. J. Mol. Biol. *324*, 807–822.

Will, C.L., and Lührmann, R. (2001). Spliceosomal UsnRNP biogenesis, structure and function. Curr. Opin. Cell Biol. *13*, 290–301.

Will, C.L., and Lührmann, R. (2006). Spliceosome structure and function. In The RNA World, Third Edition, R.F. Gesteland, T.R. Cech, and J.F. Atkins, eds. (Cold Spring Harbor, New York: Cold Spring Harbor Laboratory Press), pp. 369–400.

Yitzhaki, S., Miriami, E., Sperling, J., and Sperling, R. (1996). Phosphorylated Ser/Arg-rich proteins: Limiting factors in the assembly of 200S large nuclear ribonucleoprotein particles. Proc. Natl. Acad. Sci. USA *93*, 8830–8835.

Zhang, L., Shen, J., Guarnieri, M.T., Heroux, A., Yang, K., and Zhao, R. (2007). Crystal structure of the C-terminal domain of splicing factor Prp8 carrying retinitis pigmentosa mutants. Protein Sci. *16*, 1024–1031.

Zhao, R., Shen, J., Green, M.R., MacMorris, M., and Blumenthal, T. (2004). Crystal structure of UAP56, a DExD/H-box protein involved in pre-mRNA splicing and mRNA export. Structure *12*, 1373–1381.